RI bureau of mines
report of investigations 7404

# FACTORS RELATED TO MINERAL SEPARATION IN A VACUUM



UNITED STATES DEPARTMENT OF THE INTERIOR
BUREAU OF MINES
June 1970

# FACTORS RELATED TO MINERAL SEPARATION IN A VACUUM

By Foster Fraas

* * * * * * * * * * * * report of investigations 7404


UNITED STATES DEPARTMENT OF THE INTERIOR

BUREAU OF MINES

This publication has been cataloged as follows:

Fraas, Foster

Factors related to mineral separation in a vacuum. [Washington] U.S. Dept. of the Interior, Bureau of Mines [1970]

13 p. illus., tables. (U.S. Bureau of Mines. Report of investigations 7404)

Includes bibliography.

1. Vacuum metallurgy. I. Title. II. Title: Mineral separation in a vacuum. (Series)

TN23.U7 no. 7404 622.06173

U.S. Dept. of the Int. Library

CONTENTS



ILLUSTRATIONS



TABLES

# FACTORS RELATED TO MINERAL SEPARATION IN A VACUUM

by

Foster Fraas[1]


## ABSTRACT

Under a very high vacuum of $10^{-8}$ torr the transfer of terrestrial mineral beneficiation methods to the vacuum ambient of extraterrestrial locations such as the lunar surface was investigated. In the size range for the electrostatic and magnetic separation of ores (minus 35 plus 150 mesh) there is no adhesion of particles produced by crushing and grinding due to the limited contact area, and for repeated contacts area size has a frequency of occurrence in accordance to the normal law. The photoelectric effect which is successful in separating a few minerals in an air ambient has a wider application in a vacuum, while the lack of air viscosity and sound transmission provides for high feed velocities and the adaptation of particle vibration to dispersion and grinding. Contact electrification is reversible upon return to atmosphere.


## INTRODUCTION

This investigation has for its purpose the transfer of terrestrial mineral separation methods to the vacuum ambient of extraterrestrial locations. Mineral separation in a vacuum has never been considered before, although related information is obtained from the results of a long-range mineral beneficiation program of the Bureau of Mines including theory and application of electrostatic (6-7)[2] and magnetic (8-9, 11) separation, the magnetization delay factor (10), and effects related to changes on the mineral surface (5-12). A primary objective is the determination of the extent of the increase of particle adhesion in a vacuum and the harmful effect this may have on the flow of particles. Other objectives include changes in contact electrification and the advantages which a vacuum may provide.

---

[1]Metallurgist, College Park Metallurgy Research Center, Bureau of Mines, College Park, Md.

[2]Underlined numbers in parentheses refer to items in the list of references at the end of this report.

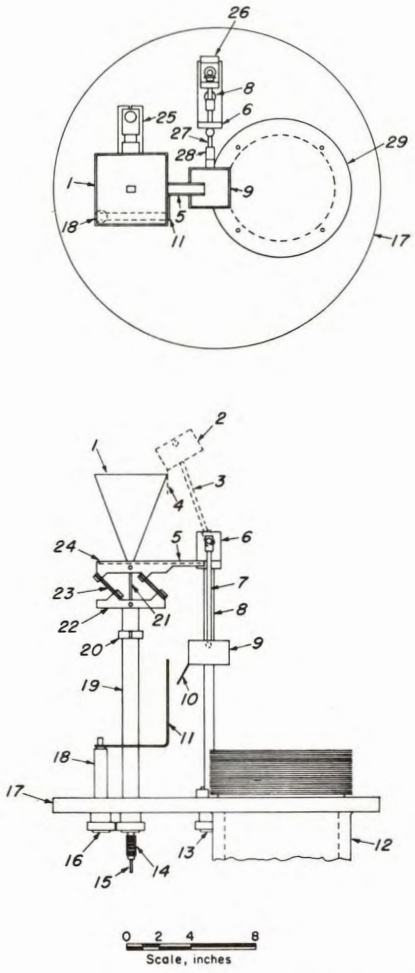


1 Feed hopper
2 Bin dumping position
3 Bin support arm
4 Trip rod dumping position
5 Feeder transport surface
6 Bearing support
7 Rotating bin support arm
8 Support column
9 Bin particle collecting position
10 Trip rod
11 Charge measurement electrode
12 Vacuum pumping port
13 Bellows type rotating feed-through
14 Bellows type vibrating feed-through
15 Rod connecting to vibration drive unit
16 Charge measurement feed-through
17 Off-center bell jar base plate
18 Low capacitance support rod
19 Hollow tube support column
20 Feed hopper support bracket
21 Vibration drive rod
22 Vibration feeder base
23 Vibrating feeder reeds
24 Vibrating portion of feeder
25 Feed hopper support bracket
26 Miter gear box
27 Horizontal shaft supporting bin
28 Porcelain insulator on shaft 27
29 Pump protection baffle

FIGURE 1. - Flow and Contact Electrification Measurement Apparatus.

## EXPERIMENTAL METHOD

### The Vacuum System

Information on the experimental arrangement may be obtained from figure 1. The Welch[3] model 3102 turbomolecular pump could be baked with heaters supplied by the manufacturer while baking of the 18- by 30-inch stainless steel bell jar was accomplished with three 385-watt heating tapes spaced on the bell jar surface. A double O-ring seal between the bell jar and base plate permitted easy opening and closing of the system. Although a seal of this type introduces limitations to the maximum attainable vacuum, satisfactory operation close to the $10^{-9}$ torr limit of the pump could be attained with Apiezon type L grease on the O-rings. This grease has a vapor pressure of $10^{-11}$ torr at room temperature. A water cooled flange on the bell jar prevented heating of the seal during bakeout. Vacuum was measured with an ionization gage and NRC 720 control, while lifting of the bell jar was facilitated with a Heraeus-Engelhard hydraulic hoist.

There is no oil contamination source except at the bearings located at the pump exhaust port. Since the pump removes all gases equally, the oil vapor which may arise at the bearings is continually exhausted. However, improper procedures, such as permitting the bell jar backfill to pass through the pump, will result in oil contamination. When the backfill, nitrogen or air, is introduced through the bell jar base plate, hydrocarbon contamination is prevented.

[3]Reference to specific brands or makes or models of equipment is made for identification only and does not imply endorsement by the Bureau of Mines.

## Contact Electrification Measurement

Particle charging occurred on the vibrating feeder which was driven by an MB model SC drive unit. By means of rotation with a rotating feed-through and a PIC model BA3 miter gear the particles collected in the bin could be returned to the feed hopper, and by a reverse rotation, as illustrated in figure 1, the bin could be brought into contact with an insulated electrode for potential measurement with a Keithley model 220 electrometer. Capacitance of the electrical system was determined by measuring the change in potential with change in capacitance resulting from an added standard variable capacitance. The pump was protected from falling particles by a baffle of 24 stainless steel rings constructed of 0.02-inch-thick sheet and spaced 0.10 inch apart.

## Experimental Procedure

The procedure for vacuum operation was first to pump with an 18-hour bakeout period, next to cool to atmospheric temperature, and then to backfill with air for sample addition. This initial bakeout of the system was found to provide at room temperature a higher vacuum in a shorter pumping time. Pumping at room temperature was resumed for 2-1/2 more hours, after which the first pass of the sample under vacuum was conducted. The second pass over the vibrating feeder was also conducted at room temperature, but with an intervening 18-hour bakeout period during which the temperature of the sample in the feed hopper was raised to 100°-104° C, near the maximum[4] which might be encountered. Illumination for observation through a sight port was supplied by an 18-ampere, 6-volt projection lamp bulb with its base removed.

# EXPERIMENTAL RESULTS

## Particle Flow and Dispersion

Through a sight port in the bell jar it was observed that with a vacuum of $6 \times 10^{-8}$ to $8 \times 10^{-8}$ torr a flow of minus 35- plus 65-mesh particles occurred without adhesion to the vibrating feeder or the collecting bin even though the sample was returned to the feed hopper and repassed. In the minus 65- plus 150-mesh range an adhering single-particle layer occurred on the vibrating feeder near the feed hopper and at the discharge end. The particle sizes cover the range adaptable to electrostatic and dry magnetic separation.

The particles were fragments produced by crushing and grinding. For adhesion at these granular sizes surface contour is of prime importance. Particle adhesion when it does occur requires either polished dust free surfaces or very small particle sizes. An illustrative calculation on molecular force adhesion has been made by Lowe (17). Although Wagner (28) demonstrated adhesion of 6-mm-diameter optically polished spheres in a vacuum of $10^{-9}$ torr, other data in the literature show that similar adhesion, including particle-to-particle adhesion, occurs at atmospheric pressure for sand sizes. This fact

[4] According to Penn (20) the temperature of the lunar environment varies from -148° to +102° C.

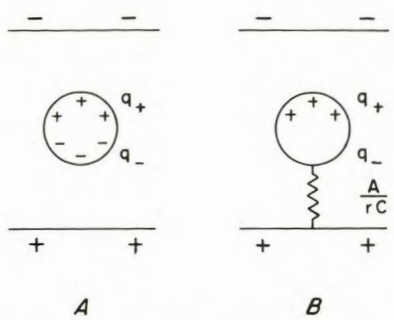


FIGURE 2. - Particle Charging and Discharging Relations.

has been demonstrated previously (6, p. 61), wherein dry beach sand with a surface contour similar to rounded gravel was found to agglomerate when stirred with a glass rod. Since the agglomeration disappeared on exposure to an alternating current corona, the attractive forces were identified as electrostatic. On rounded particles of this type the total attainable contacting area is close to that calculated from the particle dimensions.

For fragmented particles contact area is limited to the surface peaks and for repeated contacts an assortment of contact areas would be obtained. It can be shown that the frequency of occurrence of a specific contact area is in accordance to the normal law. The procedure involves charge accumulation measurements as electrically conductive particles pass over an electrode.

As illustrated in figure 2A an uncharged particle when placed in an electric field will acquire the induced charges, $q_-$ and $q_+$, whose sum is equal to zero. In figure 2B the particle is brought into contact with one of the electrodes which produce the field, and the particle charge adjacent to the electrode flows across the contact area, A. If this transferable charge is $q_-$ and is discharged completely, the total charge on the particle changes from $(q_- + q_+)$ to $q_+$. The relation between q and the contact area is therefore represented by the discharge of a condenser, where C is the capacitance of the condenser system contributed by the particle, E is the potential across the contact area, and r is the specific resistivity of the particle. For the discharge of a condenser,

$$\frac{dq}{q} = -\frac{A}{rC}\,dt, \tag{1}$$

where t is the time. Integrating and solving for the integration constant at t = o,

$$\log q = \frac{-At}{rC} + \log CE. \tag{2}$$

Since in the charge measurements the electric field intensity is sufficiently low to eliminate electrostatic deflection, t is a constant. C is a constant when the particle diameter is constant. The negative sign in equations 1 and 2 appears from the rate of change of charge with respect to change in time. Equation 2 may accordingly be rewritten

$$\log q - \log CE = \log nQ - \log CE = A\left(\frac{-t}{rC}\right), \tag{3}$$

where Q is the measured charge in arbitrary units after the particle leaves the field, n is a constant, and q is the actual charge on the particle.

Data of this type represented as a straight-line cumulative percentage plot have been presented (6, p. 43). Differentiation through the use of Fry's table (13, p. 456) provides a frequency of occurrence plot as illustrated in figure 3. The mean charge, log $Q_m$ is equal to 0.4, and the equivalent area may be found by the equation

$$\log nQ - \log nQ_m = \log Q - \log Q_m = (A-A_m)\left(\frac{-t}{rC}\right). \quad (4)$$

The term on the right side of equation 4 is a function of the actual area A. Over the theoretical range in figure 3 this function has an approximate eightfold variation.

## Contact Electrification

The successive contact electrification measurements are summarized in table 1. The final weight of sample in the bin after return to atmosphere was less than the initial weight. Loss of sample is due to the higher bounce of the particles in vacuum, there being under these conditions no restraint to particle movement such as that which results from the viscosity of ambient air. The actual increase in rebound distance will be described later.

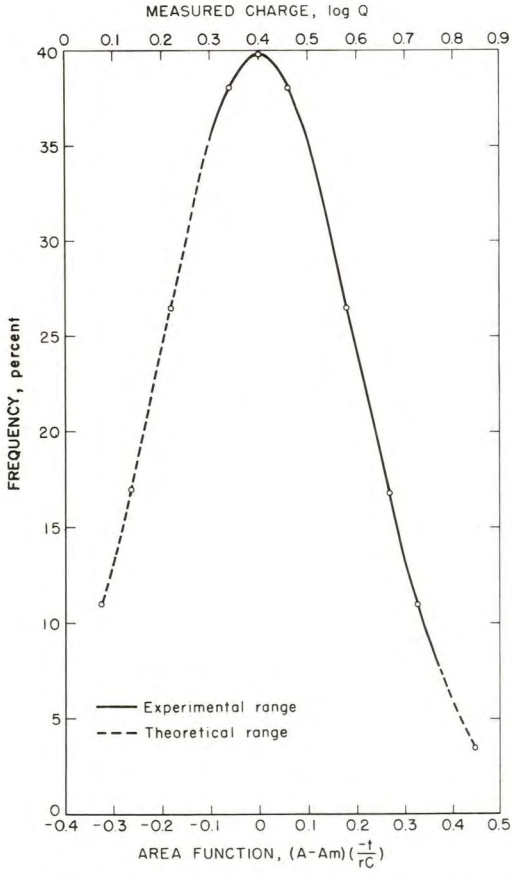


FIGURE 3. - Frequency of Occurrence of Particle Contact Area.

After contact electrification was measured in the atmosphere, the 2-gram sample was returned to the feed hopper (1, fig. 1). With this operation there was no loss of particles by bouncing. The average charge on the particle was calculated on the basis of a measured electric capacitance of $83 \times 10^{-12}$ farad for the bin, feed-through, and electrometer. The low value for the average charge is attributed to several factors. One is that the vibration intensity of the feeder is too low for satisfactory charging for contact electrification separation; another is that the average charge is calculated from the bulk charge and, as known from contact electrification studies (6), some particles acquire a charge polarity opposite to the bulk polarity.

Examination of table 1 indicates that the contact electrification for the first pass under vacuum is greater than that in air. This can be attributed to both the absence of a corona leakage discharge, which can occur in air, and the absence of surface conductivity due to atmospheric moisture (6). Parks (19) has presented an excellent theory with

confirming data on the effect of $H_2O$ adsorption on surface conductivity and contact electrification.

TABLE 1. - Contact electrification of minerals in vacuum and in air

| Mineral | Particle size,[1] mesh | Initial atmospheric pass, volts[2] | First pass under vacuum[3] | | Second pass under vacuum[4] | | Pass after return to atmosphere | | |
|---|---|---|---|---|---|---|---|---|---|
| | | | Volts | Average particle charge, coulombs $\times 10^{14}$ | Actual volts | Corrected[5] volts | Weight, g[5] | Actual volts | Corrected[5] volts |
| Microcline... | -35 + 65 | -3.6 | -12 | 1.8 | -6.4 | -7.7 | 1.660 | - | - |
| | -65 + 150 | -11 | -29 | 1.3 | -34 | -43 | 1.574 | -8.5 | -11 |
| Olivine..... | -35 + 65 | +7.0 | +10 | 2.0 | +10 | +16 | 1.288 | +5.0 | +7.8 |
| | -65 + 150 | +6.0 | +6.3 | .21 | +8.0 | +11 | 1.526 | +10 | +13 |
| Hornblende... | -35 + 65 | -8.6 | -9.0 | 1.7 | -5.5 | -10 | 1.033 | -4.2 | -8.1 |
| | -65 + 150 | -16 | -40 | 1.4 | -26 | -31 | 1.659 | -15 | -18 |
| Quartz..... | -35 + 65 | -18 | -64 | 9.5 | -34 | -39 | 1.754 | -42 | -48 |
| | -65 + 150 | -14 | -42 | 1.8 | -36 | -39 | 1.867 | -12 | -13 |

[1] Standard screen scale. Mesh sizes 35, 65, and 150 correspond to sieve openings of 420, 210, and 104 microns, respectively.

[2] Initial weight of sample = 2.00 grams.

[3] First pass at room temperature with no intervening increase in temperature. Vacuum values for succeeding data down column were 4.6, 5.5, 7.2, 4.9, 4.0, 4.2, 4.3, and $4.0 \times 10^{-7}$ torr.

[4] Second pass conducted at room temperature but with an intervening 18-hour sample temperature of 102°±2° C. Vacuum values for succeeding data down column were 8.0, 7.6, 7.8, 7.8, 7.6, 6.1, 6.8, and $7.5 \times 10^{-8}$ torr.

[5] Corrected volts are for 2.0 grams calculated from weight after return to atmosphere.

Correction for loss of weight indicates that upon return to atmosphere the electrification potentials are reversible for all minerals except the fine size olivine and the coarser size quartz. Since the coarse particle size tests were conducted during the winter low humidity period the high electrification of the quartz after return to atmosphere may be attributed to a lag in $H_2O$ readsorption. The fine particle size tests were conducted during the summer when the relative humidity was 50±5 percent at 28°±2° C. The higher potential for the fine size olivine upon return to atmosphere may be explained on the basis that the relative humidity was 54 percent at 26° C for the initial pass, and 45 percent at 26° C after return to atmosphere.

Except for the fine size microcline and the coarse size hornblende there is a trend to more positive contact electrification values between the first and second passes in vacuum. At the low temperature and short time of the bakeout any changes which may occur can only be attributed to the desorption of high vapor pressure substances which may include water.

A vibrating feeder with a contacting surface more negative in contact potential value than the aluminum used in these tests would decrease the magnitude of the microcline, hornblende, and quartz negative charges and might change them to positive electrification polarities. It has previously been shown (6) that when a number of nonconductive minerals and electrically conductive contact surfaces are alternately arranged in a series according to contact electrification polarities, the conductive contact surfaces are automatically arranged in a contact potential series.

By inference the nonconductive minerals are also arranged in a contact potential series. Contact potential theory is based on the flow of electrons in metals and the energy required to remove them from the Fermi level. For an extension to nonconductors Vick (27) postulated the existence of lattice imperfections on the nonconductor surface.

At temperatures sufficiently higher than 100° C, contact electrification upon return to atmosphere would not be reversible because of the changes in the lattice imperfections at the surface. It has previously been shown (6, p. 64) that beryl when heated to 500° C loses cations from its surface with a change from positive to negative contact electrification. The cations could be restored by treatment in solutions of NaOH and $NH_4OH$. Restoration to a positive electrification polarity can also be accomplished by an electrical discharge in hydrogen (12).

## Advantages of Vacuum Operation

Vacuum operation eliminates the factors related to air, viscosity, the transmission of sound, and the restrictions to the transmission of electromagnetic radiation and atomic particles.

### Air Viscosity

Air viscosity may either stop a particle having an initial velocity, or limit the maximum velocity which a particle attains under acceleration by gravity. The stopping distance, s, can be calculated by the use of $\tau$, the time-of-flight factor. If the initial velocity of the particle is v, then the stopping distance is

$$s = \tau v. \tag{5}$$

For particles which follow Stokes' law, $\tau$ can be calculated theoretically. For the case in which the theoretical conditions do not hold because of changes in the Reynolds' number due to turbulence, Davies (4) has presented a table of values. The same table supplies terminal velocities, v, for particles falling in air.

An unexpected high bounce of particles in vacuum has been noted. Comparison with the rebound in air may be calculated with the use of the above data and the equations

$$s = 1/2\ gt^2 \tag{6}$$

and

$$v = gt, \tag{7}$$

where g is the acceleration of gravity and t is the time. Rebound calculations in air and vacuum are summarized in table 2.

TABLE 2. - Rebound comparison of a 200-micron particle[1]

| Flight factors | Air ambient | Vacuum ambient |
|---|---|---|
| Fall distance, cm[2] | 16.4 | 16.4 |
| $\tau$, seconds[3] | $7.14 \times 10^{-2}$ | $\infty$ |
| v, cm per second[4] | 70 | 180 |
| Rebound distance, cm | 5 | 16.4 |

[1] Spherical particle of unit density.
[2] Distance from feeder to collecting bin.
[3] Data of Davies (4).
[4] Terminal velocity of fall.

## Sound Transmission

The much higher velocities of fall which a particle can attain in a vacuum result in much higher intensities of resonating vibrations initiated by the elastic deformation of the particle during rebound. The vacuum also reduces sound radiation losses to zero. At the small particle sizes where the sound radiation losses in air become prohibitive, there is an increased possibility for stored energy because of the less likely occurrence of cracks and polycrystalline structure.

The total energy of a system is the sum of the potential and kinetic energies and is equal to the kinetic energy when this is a maximum. The increment in energy, $\partial w$, in a layer of unit area of incremental thickness, $\partial x$, is

$$\partial w = \tfrac{1}{2} \rho \, \partial x \left( \frac{d\xi}{dt} \right)^2. \tag{8}$$

where $\rho$ is the density of the medium (29). When the kinetic energy is a maximum, the rate of displacement of medium, $\frac{d\xi}{dt}$, is a maximum. At the maximum in simple harmonic motion,

$$\frac{d\xi}{dt} = 2\pi f a, \tag{9}$$

where f is the frequency and a is the amplitude of vibration. For unit volume, equation 8 at the maximum kinetic energy becomes

$$w = \tfrac{1}{2} \rho (2\pi f a)^2. \tag{10}$$

With the sound waves reflected back from the surface of a solid cube of dimension z and density $\rho_s$, the retained sound is the stored energy represented by

$$w = \tfrac{1}{2} \rho_s (2\pi f a)^2 z^3. \tag{11}$$

When the cube particle is placed in air with a density $\rho_a$ and a sound velocity c, the rate of energy decrease by radiation from two opposited faces would be

$$\frac{dw}{dt} = -\tfrac{1}{2}\ \rho_a (2\pi fa)^2 c(2z^2). \tag{12}$$

Combining equations 11 and 12,

$$\frac{dw}{w} = -\frac{\rho_a}{\rho_s}\frac{2c}{z}\ dt. \tag{13}$$

Integration of equation 13 and solving for the integration constant at t = o provides the equation

$$\log w_o - \log w = \frac{\rho_a}{\rho_s}\frac{2c}{z}\ t, \tag{14}$$

where $w_o$ is the initial stored energy at t = o and w is the stored energy after an elapse of time. With a constant elapse of time the loss of energy increases with decrease in the particle dimension z. We therefore conclude that for small particles resonating vibrations will be retained much longer with a vacuum ambient than an air ambient.

The large intensities of stored resonating energy resulting from the rebound of particles falling from a great height in vacuum would contribute to the dispersion of agglomerates and the removal of dust from the particle surface. Piezoelectric properties of the particles, of which 20 of the total of 32 crystal classes are piezoelectric (21), provide for electromechanical coupling (25). Application of an external resonating electric field would accentuate the vibrations to increase dispersion and provide means for particle size reduction by fracture, particularly at the grain boundary of two locked minerals.

## Radiation Transmission

A vacuum ambient permits the unrestricted transmission of electromagnetic radiation and atomic particles. Of particular interest is ultraviolet radiation which has a high absorption in air at wavelengths less than 2,000 A (24). That the photoconductive effect can be adapted to the separation of minerals was demonstrated in air with the equipment shown in figure 4. Here the amount of sphalerite particles collected in the conductor fraction bin changed from 8 to 91 percent of the total feed when the particles on the separator roll were irradiated with ultraviolet light from a high-pressure quartz envelope lamp.

Although sphalerite is not included in the list of minerals postulated as existing on the lunar surface, Hartmann (14) measured the photoemission of silica with an electron camera. The same technique was used by others (1-2). Additional data on insulators using electric current methods include photoemission (15) and photoconductivity effects (3, 16-23, 26). In the range

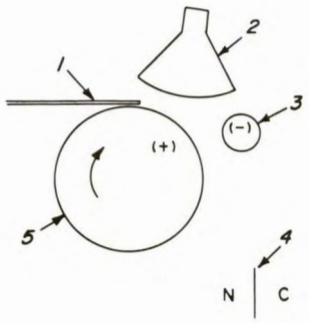


1 Vibrating feeder
2 Ultraviolet lamp
3 Cylindrical high-voltage electrode, 2-inch diameter
4 Dividing edge. Conductor particles arrive at C and nonconductor particles arrive at N
5 Ground potential cylindrical rotating roll, 6-inch diameter

FIGURE 4. - Apparatus for Photoelectric Mineral Separation.

20 to 120 A two photoemission peaks occur near 100 A for BeO (24).

Photoactivation may be supplemented to some extent by thermal activation. This is illustrated in table 3 with diamond. For a conductive response in an electrostatic separator the contact resistance should be $10^{12}$ ohms or less (7). Since the number of photoconductors is proportional to the square root of the light intensity (18), a lamp with at least 100 times the intensity would be required for a resistance of $10^{12}$ ohms at 50° C.

Atomic particles in the form of electrons from a heated cathode, or positive ions such as hydrogen ions, would have application in the electrostatic separation of conductors from nonconductors. In terrestrial applications this separation is carried out with an air ionizing electrode (6). An alternative application of electrons or positive ions when deposited on particle surfaces is the dispersion of agglomerates by the repelling effect of similar charges.

TABLE 3. - Results of supplementing photoactivation with thermal activation[1]

| Treatment | Temperature, ° C | Contact resistance, ohms |
|---|---|---|
| None..... | 50 | $10^{16}$ |
| None..... | 200 | $10^{13}$ |
| Irradiated[2]..... | 50 | $10^{13}$ |
| Irradiated[2]..... | 200 | $10^{12}$ |

[1] Contact resistance of a 200-micron diamond particle using the method previously described (6, p. 69) with 200 volts across the electrodes.
[2] Irradiation from a Continental Lithograph Corporation H4 high-pressure quartz lamp.

## CONCLUSIONS

With particles produced by crushing and grinding there will be no difficulty in the electrostatic and magnetic separation of minerals in a vacuum, provided separation is confined to particles coarser than 150 mesh. The lack of air viscosity permits magnetic and electrostatic separation at high feed rates, while the absence of sound transmission in space results in a vibration method for the dispersion of particle agglomerates and the removal of particle surface dust.

Another advantage of vacuum operation is the elimination of the ultraviolet absorption which occurs in air at wavelengths below 2,000 A. At the shorter wavelengths photoconductive and photoemission effects may be useful in increasing the selectivity of mineral separation. The increased electrical insulation of a vacuum provides for larger contact electrification charges and higher electrical operating potentials, both of which would contribute to electrostatic separation at larger particle sizes. Even though the air ionizing electrode, normally employed in the electrostatic separation of conductors from nonconductors, will not operate in a vacuum, the same separation can be accomplished by the use of electrons from a heated cathode, or by the use of positive ions such as hydrogen ions. A secondary effect of ion deposition is the dispersion of particle agglomerates.

## ACKNOWLEDGMENT

The author wishes to acknowledge the support of the Office of Advanced Research and Technology, National Aeronautics and Space Administration. The research was conducted as part of the Bureau of Mines program of Multidisciplinary Research Leading to Utilization of Extraterrestrial Resources under NASA contract R-09-040-001.

## REFERENCES[5]


1. Bizouard, M., and J. Crousillat. Emission photoélectrique de monocristaux de KCl et de KI (Photoelectric Emission of Single Crystals of KCl and KI). C. R. Acad. Sci., v. 263, No. 22, Nov. 27, 1967, pp. 1263-1264.

2. Bizouard, M., J. Pantaloni, and J. Crousillat. Emission photoélectrique d'un monocristal de NaCl (Photoelectric Emission of a Single Crystal NaCl). C. R. Acad. Sci., v. 262, No. 4, Jan. 24, 1966, pp. 278-280.

3. Cook, J. R. Photoconductivity in Calcium Tungstate. Proc. Phys. Soc., v. B68, January 1955, pp. 148-155.

4. Davies, C. N. Aerosol Science. Academic Press, New York, 1966, pp. 393-395.

5. Fraas, F. Calculation of Adsorption Energy. BuMines Rept. of Inv. 6639, 1965, 14 pp.

6. _____. Electrostatic Separation of Granular Materials. BuMines Bull 603, 1962, pp. 12, 43, 61, 64-65, 68-69.

7. _____. Electrostatic Separation of High Conductivity Minerals. BuMines Rept. of Inv. 6404, 1964, p. 12.

8. _____. Magnetic Separator With a Combination Field. U.S. Pat. 3,382,977, May 14, 1968.

9. _____. Magnetic Separation of Minerals of Low Susceptibility and Small Particle Size. BuMines Rept. of Inv. 7292, 1969, 14 pp.

10. _____. Magnetization Delay in the Separation of Minerals. BuMines Rept. of Inv. 6411, 1964, 13 pp.

11. _____. The Matrix Type Magnetic Separator. BuMines Rept. of Inv. 6722, 1966, 11 pp.

12. _____. Pretreatment of Minerals for Electrostatic Separation. U.S. Pat. 3,137,648, June 16, 1964.

13. Fry, T. C. Probability and Its Engineering Uses. D. Van Nostrand Company, Inc., New York, 7th ed., 1928, p. 456.

14. Hartmann, M. P. Excitation de l'emission photoélectrique de la silice par irradiation en lumiére ultraviolette (Excitation of Photoelectric Emission in Silica by Irradiation in Ultraviolet Light). C. R. Acad. Sci., v. 257 , No. 17, Oct. 21, 1963, pp. 2447-2450.


[5]Titles enclosed in parentheses are translations from the language in which the item was originally published.

15. Hughes, O. H., R. H. Tredgold, and R. H. Williams. Photoemission Studies on Barium Titanate. J. Phys. Chem. Solids, v. 27, January 1966, pp. 79-84.

16. Klein, W., G. Schatz, and K. Seeger. Ausserer Photoeffect und Verzogerte Elektronenmission von Ultraviolettbestrahlten KCl and KBr Einkristallen (Photoeffect and Retarded Electron Emission of Ultraviolet Irradiated KCl and KBr Single Crystals). Z. Phys., v. 160, 1960, pp. 443-452.

17. Lowe, H. J., and D. H. Lucas. The Physics of Electrostatic Precipitation. British J. Appl. Phys., Suppl. 2, March 1953, p. S45.

18. Mott, N. F., and R. W. Gurney. Electronic Processes in Electronic Crystals. Oxford Univ. Press, London, 1953, p. 123.

19. Parks, G. A., B. K. Jindal, and J. H. Anderson, Jr. Temperature and Humidity in Electrical Separation of Oxide Minerals. Trans. AIME, v. 235, December 1966, pp. 451-457.

20. Penn, S. H. An Experimental Investigation Simulating the Behavior of a Rock-Drill on the Lunar Surface. Trans. AIME, v. 238, March 1967, pp. 72-82.

21. Pugh, S. F., and P. J. Anderson. Electrostriction and Piezoelectricity. Encyclopaedic Dictionary of Physics, The MacMillan Company, New York, v. 2, 1962, p. 837.

22. Randall, J. T., and M. H. F. Wilkins. The Phosphorescence of Various Solids. Proc. Roy. Soc. London, v. A184, Nov. 6, 1945, pp. 348-364.

23. Reiber, K., and A. Scharmann. Photoleitfahigkeit von $CaWO_4$ Einkristallen (Photoconductivity of $CaWO_4$ Single Crystal). Z. Phys., v. 191, 1966, pp. 480-486.

24. Samson, J. A. R. Techniques of Vacuum Ultraviolet Spectroscopy. John Wiley & Sons, Inc., New York, 1967, pp. 1, 232.

25. Stokes, R. G. An Improved Apparatus for Detecting Piezoelectricity. Am. Miner., v. 32, Nos. 11-12, November-December 1947, pp. 670-677.

26. Taylor, J. W., and P. L. Hartmann. Photoelectric Effects in Certain of the Alkali Halides in the Vacuum Ultraviolet. Phys. Rev., v. 113, Mar. 15, 1959, pp. 1421-1435.

27. Vick, F. A. Theory of Contact Electrification. British J. Appl. Phys., Suppl. 2, March 1953, pp. S1-S5.

28. Wagner, P. E. Electrostatic Charge Separation at Metal-Insulator Contacts. J. Appl. Phys., v. 27, No. 11, November 1956, pp. 1300-1311.

29. Wood, A. B. Textbook of Sound. Dover Publications Inc., New York, 3d ed., 1955, 610 pp.

INT.-BU.OF MINES,PGH.,PA. 14966